

# Nielsen Thermal Conductivity Model for Single Filler Carbon/Polypropylene Composites

Daniel Lopez Gaxiola, Jason M. Keith, Julia A. King, Beth A. Johnson

Department of Chemical Engineering, Michigan Technological University, Houghton, Michigan 49931-1295

Received 2 December 2008; accepted 23 March 2009

DOI 10.1002/app.30484

Published online 7 August 2009 in Wiley InterScience (www.interscience.wiley.com).

**ABSTRACT:** In this study, three different carbon fillers (Thermocarb TC-300 synthetic graphite, Ketjenblack EC-600 JD carbon black, and Hyperion Catalysis International's FIBRIL™ carbon nanotubes) were added to a polypropylene matrix to produce single filler composites with filler concentrations of up to 80 wt % synthetic graphite (61.6 vol %), 15 wt % carbon black (8.1 vol %), and 15 wt % carbon nanotubes (7.4 vol %). The through-plane thermal conductivity for each formulation was measured. For the synthetic graphite, carbon black, and carbon nanotubes

composites, the Nielsen model was applied to the experimental through-plane thermal conductivity data. The Nielsen Model presented in this work showed very good agreement with experimental data. The model parameters were similar to those used in the literature for these fillers in other polymers. © 2009 Wiley Periodicals, Inc. *J Appl Polym Sci* 114: 3261–3267, 2009

**Key words:** composites; thermal properties; fillers; modeling; polypropylene

## INTRODUCTION

Most polymer resins are thermally insulating. One emerging market for thermally conductive resins is for bipolar plates for use in fuel cells. The bipolar plate separates one cell from the next, with this plate carrying hydrogen gas on one side and air (oxygen) on the other side. Hydrogen reacts with oxygen from the air to produce DC electricity. The byproducts of the reaction are heat and water. Bipolar plates require high thermal conductivity (to conduct away the generated heat), low gas permeability, and good dimensional stability.

Typical thermal conductivity values in W/m K for some common materials are 0.2 to 0.3 for polymers, 234 for aluminum, 400 for copper, and 600 for graphite. One approach to improving the thermal conductivity of a polymer is through the addition of a conductive filler material, such as carbon and metal.<sup>1–14</sup> In a polymer containing conductive fillers, heat is transferred by two mechanisms, lattice vibrations (major contributor) and electron movement.<sup>2</sup> Typically, a single type of carbon is used in thermosetting resins (often a vinyl ester) to produce a thermally conductive bipolar plate material with a desired thermal conductivity of at least 20 W/m

K.<sup>15–18</sup> Thermosetting resins cannot be remelted. Lately, carbon filled thermoplastic resins [i.e., polypropylene (PP), liquid crystalline polymer, polyphenylene sulfide, polyethylene] are being considered for fuel cell bipolar plates.<sup>19–23</sup>

In this work, researchers performed compounding runs followed by injection molding and thermal conductivity testing of carbon/PP composites. PP has been studied by several researchers for possible use for fuel cell bipolar plates.<sup>19,24</sup> PP is a semicrystalline thermoplastic that can be remelted and used again. Three different carbon fillers [electrically conductive carbon black, synthetic graphite (SG) particles, and carbon nanotubes] were studied. Composites containing varying amounts of a single type of carbon filler were fabricated and tested for thermal conductivity.

## MATERIALS AND METHODS

### Materials

The matrix used for this project was Dow's (Midland, MI) semicrystalline homopolymer PP resin H7012-35RN. The properties of this polymer are shown in Table I.<sup>25</sup> The first filler used in this study was Ketjenblack EC-600 JD, carbon black (referred to here as CB). This is an electrically conductive CB available from Akzo Nobel (Chicago, IL). The highly branched, high surface area CB structure allows it to contact a large amount of polymer, which results in improved electrical conductivity at low CB concentrations (often 5–7 wt %). The properties of

Correspondence to: J. M. Keith (jmkeith@mtu.edu).

Contract grant sponsor: National Science Foundation; contract grant number: DMI-0456537.

Contract grant sponsor: Department of Energy; contract grant number: DE-FG36-08GO88104.

**TABLE I**  
Properties of Dow's H7012-35RN PP Resin<sup>25</sup>

Melting point	163°C
Glass transition temperature	-6.6°C
Melt flow rate (230°C/2.16 kg)	35 g/10 min
Density	0.9 g/cc
Tensile strength at yield	34 MPa
Tensile elongation at yield	7%
Flexural modulus	1420 MPa
Notched Izod impact	25 J/m
Deflection temperature under load at 0.45 MPa, unannealed	110°C

Ketjenblack EC-600 JD are given in Table II.<sup>26</sup> According to the vendor literature, CB is sold in the form of pellets that are 100  $\mu\text{m}$ –2 mm in size and, upon mixing into a polymer, easily separates into primary aggregates 30–100 nm long.<sup>26</sup> A diagram of the CB structure is shown in vendor literature<sup>26</sup> and prior work from our group.<sup>27</sup> It is noted that the thermal conductivity of pure CB cannot be measured because of the small size of the aggregates.

Table III shows the properties of Asbury Carbons' (Asbury, NJ) Thermocarb TC-300, which is a SG that was previously sold by Conoco (Houston, TX).<sup>28,29</sup> Thermocarb TC-300 is produced from a thermally treated, highly aromatic petroleum feedstock and contains very few impurities. Figure 1 shows a photomicrograph of this SG.

Hyperion Catalysis International's (Cambridge, MA) FIBRIL<sup>TM</sup> nanotubes were the third filler used in this study. This is a conductive, vapor-grown, multiwalled carbon nanotube. They are produced from high-purity, low-molecular-weight hydrocarbons in a proprietary, continuous, gas-phase, catalyzed reaction. The outside diameter of the tube is 10 nm and the length is 10  $\mu\text{m}$ , which gives an aspect ratio (length/diameter) of 1000. Due to this high aspect ratio, very low concentrations of nanotubes are needed to produce an electrically conductive composite. This material was provided by Hyperion Catalysis International in a 20 wt % FIBRIL in PP masterbatch MB3020-01. Table IV<sup>30</sup> shows the properties of this filler (referred to here as CNT).

**TABLE II**  
Properties of Akzo Nobel Ketjenblack EC 600-JD CB<sup>26</sup>

Electrical resistivity	0.01–0.1 $\Omega\text{ cm}$
Aggregate size	30–100 nm
Specific gravity	1.8 g/cm <sup>3</sup>
Apparent bulk density	100–120 kg/m <sup>3</sup>
Ash content, max	0.1 wt %
Moisture, max	0.5 wt %
Brunauer–Emmett–Teller (BET) surface area	1250 m <sup>2</sup> /g
Pore volume	480–510 cm <sup>3</sup> /100 g

**TABLE III**  
Properties of Thermocarb TC-300 SG<sup>28,29</sup>

Carbon content, wt %	99.91
Ash, wt %	<0.1
Sulfur, wt %	0.004
Density, g/mL	2.24
BET surface area, m <sup>2</sup> /g	1.4
Thermal conductivity at 23°C, W/m K	600 in "a" crystallographic direction
Electrical resistivity of bulk carbon powder at 150 psi, 23°C, parallel to pressing axis, $\Omega\text{ cm}$	0.020
Particle shape	Acicular
Particle aspect ratio	1.7
Sieve Analysis, wt %	
+600 $\mu\text{m}$	0.19
+500 $\mu\text{m}$	0.36
+300 $\mu\text{m}$	5.24
+212 $\mu\text{m}$	12.04
+180 $\mu\text{m}$	8.25
+150 $\mu\text{m}$	12.44
+75 $\mu\text{m}$	34.89
+44 $\mu\text{m}$	16.17
-44 $\mu\text{m}$	10.42

### Test specimen fabrication

For this entire project, the fillers and PP were used as received. The extruder used was an American Leistritz Extruder Corporation (Somerville, NJ) Model ZSE 27. This extruder has a 27-mm corotating intermeshing twin screw with 10 zones and a length/diameter ratio of 40. The screw design, which is shown elsewhere,<sup>31</sup> was chosen to obtain a minimum amount of filler degradation, while still dispersing the fillers well in the polymers. Per the vendor's recommendation, the pure PP pellets and the Hyperion FIBRIL (CNT) masterbatch MB3020-01 (PP polymer containing 20 wt % carbon nanotubes<sup>30</sup>) were introduced in Zone 1. Per the vendor's recommendation, SG and CB were added into the polymer melt at Zone 5. Schenck (Whitewater, WI) AccuRate

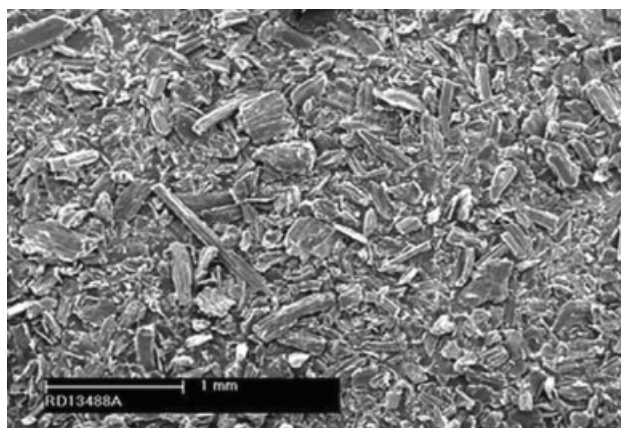


**Figure 1** Photomicrograph of Thermocarb TC-300 SG (courtesy of Asbury Carbons).

**TABLE IV**  
**Properties of FIBRIL Carbon Nanotubes<sup>30</sup>**

Composition	Pure carbon
Diameter	0.01 $\mu\text{m}$
Length	10 $\mu\text{m}$
Morphology	Graphitic sheets wrapped around a hollow 0.005- $\mu\text{m}$ core
BET (N <sub>2</sub> ) surface area	250 m <sup>2</sup> /g
Density	2.0 g/cm <sup>3</sup>

gravimetric feeders were used to accurately control the amount of each material added to the extruder.

After passing through the extruder, the polymer strands (3 mm in diameter) entered a water bath and then a pelletizer that produced nominally 3-mm-long pellets. After extrusion, PP-based composites were dried in an indirect heated dehumidifying drying oven at 80°C for 4 h and then stored in moisture barrier bags prior to injection molding.

A Niigata (Itasca, IL) injection molding machine, model NE85UA<sub>4</sub>, was used to produce test specimens. This machine has a 40-mm-diameter single screw with a length/diameter ratio of 18. The lengths of the feed, compression, and metering sections of the single screw are 396, 180, and 144 mm, respectively. A four-cavity mold was used to produce 3.2-mm-thick 6.4-cm-diameter disks (end gated).

#### **SG length, aspect ratio, and orientation test method**

To determine the length and aspect ratio (length/diameter) of the SG in the injection molded test specimens, xylene at 120°C was used to dissolve the polymer matrix. The fillers were then dispersed onto a glass slide and viewed using an Olympus (Center Valley, PA) SZH10 optical microscope with an Optronics Engineering (Goleta, CA) LX-750 video camera. The filler images (at 70 $\times$  magnification) were collected by using Scion (Frederick, MD) Image Version 1.62 software. The images were then processed using Adobe (San Jose, CA) Photoshop 5.0 and the Image Processing Tool Kit version 3.0. The length and aspect ratio of each particle was measured. For each formulation,  $\sim$  1000 particles were measured. Due to their small size, the CB (primary aggregates 30–100 nm long) and CNT (diameter of 0.01  $\mu\text{m}$  and length of 10  $\mu\text{m}$ ) could not be separated from the filter paper in the solvent digestion process; hence, this method could not be used to analyze the length and aspect ratio of CB and carbon nanotubes.

To determine the orientation of the SG in the injection-molded test specimen, a polished composite sample was viewed by using an optical microscope. For the through-plane thermal conductivity samples, the center portion was cut out of a disk and then

mounted in epoxy so that through the sample thickness (3.2 mm) the face could be viewed. The samples were then polished and viewed by using an Olympus BX60 reflected light microscope at a magnification of  $\times$ 200. The images were then processed by using Adobe Photoshop 5.0 and the Image Processing Tool Kit Version 3.0. For each formulation, the orientation was determined by viewing typically 1000 particles. Once again, due to the extremely small size of the CB and CNT, optical microscopy was not used to determine the orientation of these fillers.

#### **Thermal conductivity: Guarded heat flow meter test method**

The through-plane thermal conductivity of a 3.2-mm-thick, 5-cm-diameter disk-shaped test specimen (cut from the center of a 6.4-cm-diameter disk) was measured at 55°C (as close to ambient temperature as can be measured while still maintaining a temperature gradient in the apparatus) by using a Holometrix (Burlington, MA) Model TCA-300 Thermal Conductivity Analyzer, according to the ASTM F433 guarded heat flow meter method.<sup>32</sup> For each formulation, at least four samples were tested.

#### **Field emission scanning electron microscope test method**

A Hitachi (Pleasanton, CA) cold field emission scanning electron Microscope was used to view the fracture surface of the CB/SG/CNT/PP composite at 5 kV. This method was used to view the smaller fillers (CNT and CB) that could not be seen in the optical microscope.

## **RESULTS**

### **Sample fabrication results**

The concentrations (shown in wt % and the corresponding vol %) for the single filler composites tested in this research are shown in Table V. Increasing filler amount increases composite melt viscosity. Hence, slightly higher injection molding temperatures were used for highly filled composites. The maximum single filler amounts that could be extruded and injection molded were 80 wt % (61.6 vol %) for SG/PP composites, 15 wt % (8.1 vol %) for CB/PP composites, and 15 wt % (7.4 vol %) for CNT/PP composites. Because this project focuses on producing highly conductive composites, loading levels were chosen so that the filler amounts would produce conductive composites, while still allowing the composite material to have a sufficiently low enough viscosity to be extruded and injection molded into test specimens.

**TABLE V**  
**Single Filler Loading Levels in PP and Through-Plane Thermal Conductivity Results**

Formulation	Filler (wt %)	Filler (vol %)	Through-Plane Thermal Conductivity (W/m K)
PP	0.0	0.0	0.206 ± 0.002, <i>n</i> = 4
PP replicate	0.0	0.0	0.203 ± 0.002, <i>n</i> = 4
2.5CB	2.5	1.27	0.221 ± 0.004, <i>n</i> = 5
2.5CB replicate	2.5	1.27	0.225 ± 0.002, <i>n</i> = 5
4CB	4.0	2.04	0.240 ± 0.006, <i>n</i> = 4
5CB	5.0	2.56	0.251 ± 0.003, <i>n</i> = 5
6CB	6.0	3.09	0.261 ± 0.004, <i>n</i> = 4
7.5CB	7.5	3.90	0.276 ± 0.007, <i>n</i> = 4
10CB	10.0	5.26	0.298 ± 0.002, <i>n</i> = 5
15CB	15.0	8.11	0.337 ± 0.001, <i>n</i> = 5
10SG	10.0	4.27	0.234 ± 0.005, <i>n</i> = 5
15SG	15.0	6.62	0.266 ± 0.003, <i>n</i> = 4
20SG	20.0	9.13	0.292 ± 0.005, <i>n</i> = 4
25SG	25.0	11.81	0.352 ± 0.004, <i>n</i> = 4
30SG	30.0	14.69	0.438 ± 0.001, <i>n</i> = 4
35SG	35.0	17.79	0.503 ± 0.005, <i>n</i> = 4
40SG	40.0	21.13	0.628 ± 0.008, <i>n</i> = 4
45SG	45.0	24.74	0.726 ± 0.024, <i>n</i> = 4
50SG	50.0	28.66	0.896 ± 0.006, <i>n</i> = 4
55SG	55.0	32.93	1.150 ± 0.005, <i>n</i> = 4
60SG	60.0	37.60	1.494 ± 0.022, <i>n</i> = 4
65SG	65.0	42.70	1.971 ± 0.088, <i>n</i> = 4
65SG replicate	65.0	42.70	1.987 ± 0.060, <i>n</i> = 4
70SG	70.0	48.40	2.712 ± 0.049, <i>n</i> = 4
75SG	75.0	54.66	3.641 ± 0.036, <i>n</i> = 5
80SG	80.0	61.64	6.042 ± 0.098, <i>n</i> = 5
1.5CNT	1.5	0.68	0.215 ± 0.001, <i>n</i> = 5
2.5CNT	2.5	1.14	0.229 ± 0.002, <i>n</i> = 5
4CNT	4.0	1.84	0.258 ± 0.002, <i>n</i> = 4
5CNT	5.0	2.31	0.281 ± 0.002, <i>n</i> = 4
6CNT	6.0	2.79	0.302 ± 0.003, <i>n</i> = 4
6CNT replicate	6.0	2.79	0.297 ± 0.001, <i>n</i> = 4
7.5CNT	7.5	3.52	0.328 ± 0.002, <i>n</i> = 4
10CNT	10.0	4.76	0.371 ± 0.004, <i>n</i> = 4
15CNT	15.0	7.36	0.467 ± 0.004, <i>n</i> = 4

### SG filler length, aspect ratio, and orientation results

For the SG/PP composites, most of the injection-molded specimens showed a length and aspect ratio of ~ 40 and 1.67 μm, respectively. If compared to the received material and to the materials used in previous work, such as nylon, polycarbonate, and liquid crystal polymer resins, the dimensions are similar.<sup>33–35</sup>

The fillers in the through-plane samples are primarily oriented transverse to the thermal conductivity measurement direction. These observations agree with prior work and photomicrographs can be seen elsewhere.<sup>33–35</sup>

### Field emission scanning electron microscope results

The CNT (white fibers) and CB (white spheres) contained in the PP sample are shown in Figure 2. The networks formed by carbon nanotubes can be clearly observed in this figure.

### Thermal conductivity results

In Figures 3–5, the values obtained for the through-plane thermal conductivity are shown. These were measured by using the guarded heat flow meter, for the conductive resins at different concentrations of the fillers as a function of their volume fractions.

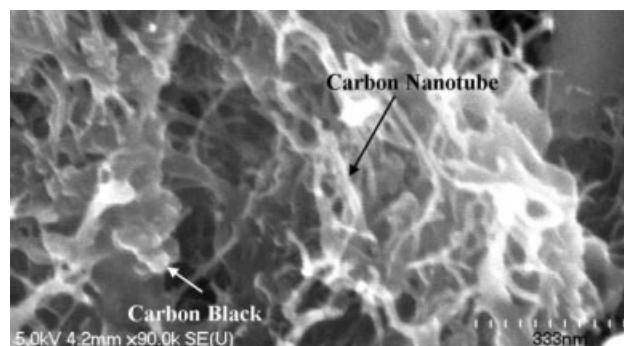


**Figure 2** Field emission scanning electron microscope photomicrograph of CB/SG/CNT in PP composite.



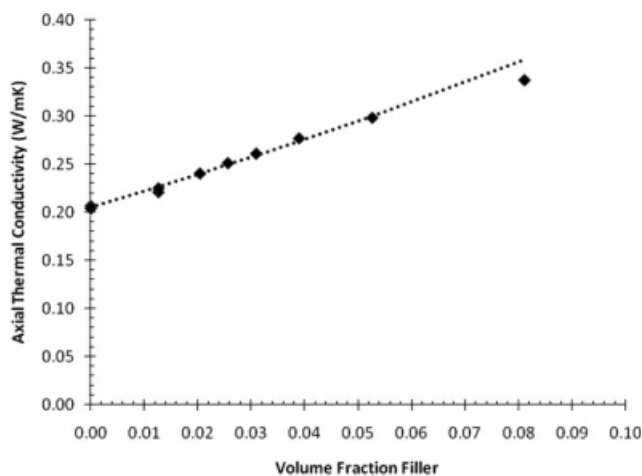


**Figure 3** Experimental (diamonds) and theoretical (line) through-plane thermal conductivities for CB/PP composites.

The corresponding formulations for these filler concentrations are shown in Table V. A standard deviation of 5% of the mean was observed for the thermal conductivity measurements.

CB had an effect of increasing the thermal conductivity of PP, ranging from 0.20 to 0.34 W/m K, at a CB concentration of 15 wt % (8.1 vol %). The thermal conductivity obtained by using CB as a filler was lower than those formed from CNT/PP composites, as seen in Figure 4. The thermal conductivity at a concentration of 15 wt % (7.4 vol %) of CNT was 0.47 W/m K.

The through-plane thermal conductivity results for different amounts of SG in PP are shown in Figure 5. For comparison purposes, at a loading of 15 wt % (6.6 vol %) filler, the thermal conductivity was 0.27 W/m K. This is lower than values obtained for CB/PP and CNT/PP composites with similar filler load-

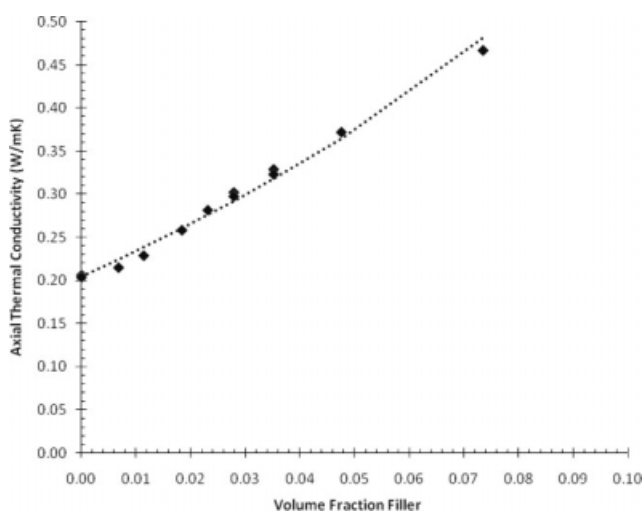


**Figure 4** Experimental (diamonds) and theoretical (line) through-plane thermal conductivities for CNT/PP composites.

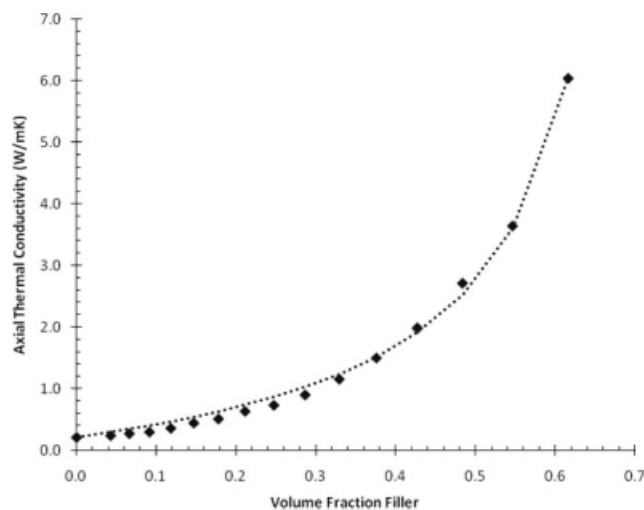


**Figure 5** Experimental (diamonds) and theoretical (line) through-plane thermal conductivities for SG/PP composites.

ings. At the highest loading of SG, 80 wt % (61.6 vol %), the thermal conductivity of the SG/PP composite was of 6.04 W/m K.

These results suggest that composites with CNT have the highest thermal conductivity due to the high filler aspect ratio. Composites with CB have a higher thermal conductivity than composites with SG due to the structure of the CB aggregates, which may help form conductive paths within the composite.

### Through-plane thermal conductivity modeling results

In this section, we use models to predict the composite thermal conductivity of carbon-filled PP composites. The most versatile is Nielsen's model, used when dealing with conductive composites formed with short fiber/particulate fillers. This model considers thermal conductivities and concentrations of each component and filler properties such as orientation, packing, and aspect ratio.<sup>36-39</sup> The next set of equations was applied for predicting the through-plane thermal conductivity  $k_{\text{through}}$  (W/m K) of the conductive resins used in this project:

$$k_{\text{through}} = k_1 \frac{(1 + AB\phi)}{(1 - B\psi\phi)} \quad (1)$$

$$B = \frac{\left(\frac{k_2}{k_1} - 1\right)}{\left(\frac{k_2}{k_1} + A\right)} \quad (2)$$

In eqs. (1) and (2), the thermal conductivity of PP is represented by  $k_1$  (W/m K);  $k_2$  (W/m K) is the thermal conductivity of the filler,  $\phi$  is the filler volume fraction,  $A$  is a factor depending on shape and orientation of the filler, and  $B$  is a factor that considers relative conductivity of both the PP and the

carbon filler. Nielsen<sup>38</sup> gives the following expression for the  $\psi$  parameter, dependent on the volume fractions of both components and  $\phi_m$ , which is the “maximum packing fraction”:

$$\psi \cong 1 + \frac{1 - \phi_m}{\phi_m^2} \phi \quad (3)$$

A standardized error,  $\varepsilon$ , was determined with eq. (4). The value obtained was used to compare experimental data with the values predicted by Nielsen’s model

$$\varepsilon = \frac{\sum_{i=1}^n (y_i - y_{\text{model}_i})^2}{\sum_{i=1}^n y_i^2}, \quad (4)$$

where  $y_i$  is the thermal conductivity result obtained from the guarded heat flow meter,  $y_{\text{model}}$  represents the value determined by using the Nielsen model, and  $i$  indicates summation of the thermal conductivities for different concentrations of the same filler. If a value of  $\varepsilon = 0$  is to be found, the experimental data will be identical to that obtained applying the model.

Nielsen’s model requires the individual thermal conductivities of the matrix and fillers. For PP we measured a thermal conductivity of 0.205 W/m K. For CB, the thermal conductivity is 2.1 W/m K.<sup>40,41</sup> For SG, the thermal conductivity is 600 W/m K.<sup>28,29</sup> For multiwalled CNT, the thermal conductivity reported in the literature ranges from 20 to 3000 W/m K.<sup>42–46</sup> As such, we will use a conservative estimate in this work of 20 W/m K.

When Nielsen’s model is applied to predict the thermal conductivity of composite materials, fixed values are assigned for the parameters  $A$  and  $\phi_m$ , which will depend on the properties of filler used, such as aspect ratio, packing fractions, and filler shape. The  $A$  values are obtained from the literature for dilute systems (low filler loading)<sup>36–38</sup> and typical values are 1.5 for spheres and less than 10 for most random fibers with aspect ratio less than 15.<sup>4,36</sup> In this research,  $A$  is allowed to be a larger value since the composite systems are highly filled. The  $A$  value used in the model is therefore an effective value for the composite.<sup>47,48</sup> The values of  $\phi_m$  are restricted to be above the maximum loading tested in our experiments and less than a larger value, which would represent an upper limit to the filler concentration that could be processed. Thus, the constraints on  $\phi_m$  were set as follows:

$$\text{Carbon Black (CB)} : 0.0811 < \phi_m < 0.20$$

$$\text{Carbon Nanotubes (CNT)} : 0.0736 < \phi_m < 0.20$$

$$\text{Synthetic Graphite (SG)} : 0.616 < \phi_m < 0.850$$

The parameters  $A$  and  $\phi_m$  used in eqs. (1)–(3) were modified by using a two-parameter optimization to minimize the standardized error calculated from eq. (4). The results found were as follows:

Carbon Black (CB) :

$$A = 70.5, \phi_m = 0.20, \varepsilon = 7.6 \times 10^{-4}$$

Carbon Nanotubes (CNT) :

$$A = 15.7, \phi_m = 0.20, \varepsilon = 7.3 \times 10^{-4}$$

Synthetic Graphite (SG) :

$$A = 8.4, \phi_m = 0.74, \varepsilon = 2.2 \times 10^{-3}$$

A comparison between experimental data and the model results is shown in Figures 3–5. In all cases, the model agrees very well with the experimental data. In comparison to previous modeling research, the  $A$  value for CB/Vectra composites ( $A \sim 1720$ )<sup>40</sup> was significantly higher than that for the CB/PP composites ( $A \sim 70$ ) but the  $\phi_m$  values were similar. For SG/Vectra composites, the  $A$  and  $\phi_m$  values were similar to those reported here ( $A \sim 8.5$ ) and ( $\phi_m \sim 0.8$ ).<sup>41,49</sup>

## CONCLUSIONS

The objective of this research project was to add three different carbon fillers (CB, CNT, and SG) to PP resins, so highly conductive composites could be produced. The concentrations of fillers in the polymer range from 1.5 up to 80 wt %. Measurements of through-plane conductivities were done for various concentrations of carbon fillers.

Theoretical values for the through-plane thermal conductivities using the three different carbon fillers were determined by applying Nielsen’s model. The model was optimized, so the values for parameters  $A$  and  $\phi_m$  would minimize the difference between experimental and model results. Thermal conductivities calculated by using Nielsen’s model were a good approximation to experimental data. In comparison to previous modeling research, the  $A$  value for CB/Vectra composites ( $A \sim 1720$ )<sup>40</sup> was significantly higher than that for the CB/PP composites ( $A \sim 70$ ) but the  $\phi_m$  values were similar. For Thermocarb/Vectra composites the  $A$  and  $\phi_m$  values were similar to those for SG/PP composites ( $A \sim 8.5$ ) and ( $\phi_m \sim 0.8$ ).<sup>41,49</sup>

The authors thank the American Leistritz technical staff for recommending an extruder screw design. The authors thank Asbury Carbons and Akzo Nobel for providing carbon fillers, Dow Chemical Company for providing the polypropylene polymer, and Albert V. Tamashausky of Asbury Carbons for providing technical advice.

## References

1. Finan, J. M. In Proceedings of the Society of Plastics Engineers Annual Technical Conference; Society of Plastics Engineers, New York, NY, 1999; p 1547.
2. Agari, Y.; Uno, T. *J Appl Polym Sci* 1985, 30, 2225.
3. Bigg, D. M. *Polym Eng Sci* 1977, 17, 842.
4. Bigg, D. M. *Polym Compos* 1986, 7, 125.
5. Bigg, D. M. *Polym Compos* 1985, 6, 20.
6. Nagata, K.; Iwabuki, H.; Nigo, H. *Compos Interfaces* 1999, 6, 483.
7. Demain, A. Ph.D. Dissertation, Universite Catholique de Louvain, Louvain-la-Neuve, Belgium, 1994.
8. King, J. A.; Tucker, K. W.; Meyers, J. D.; Weber, E. H.; Clingerman, M. L.; Ambrosius, K. R. *Polym Compos* 2001, 22, 142.
9. Murthy, M. V. In Proceedings of the Society of Plastics Engineers Annual Technical Conference; Society of Plastics Engineers, San Francisco, CA, 1994; p 1396.
10. Simon, R. M. *Polym News* 1985, 11, 102.
11. Mapleston, P. *Mod Plast* 1992, 69, 80.
12. Donnet, J.-B.; Bansal, R. C.; Wang, M.-J. *Carbon Black*, 2nd ed.; Marcel Dekker: New York, 1993.
13. Huang, J.-C. *Adv Polym Technol* 2002, 21, 299.
14. Bigg, D. M. *Polym Eng Sci* 1979, 19, 1188.
15. Wilson, M. S.; Busick, D. N. U.S. Pat. 6,248,467 (2001).
16. Loutfy, R. O.; Hecht, M. U.S. Pat. 6,511,766 (2003).
17. Braun, J. C.; Zabriskie, J. E.; Neutzler, J. K.; Fuchs, M.; Gustafson, R. C. U.S. Pat. 6,180,275 (2001).
18. Mehta, V.; Cooper, J. S. *J Power Sources* 2003, 114, 32.
19. Migri, F.; Huneault, M. A.; Champagne, M. F. *Polym Eng Sci* 2004, 44, 1755.
20. Huang, J.; Baird, D. G.; McGrath, J. E. *J Power Sources* 2005, 150, 110.
21. Wolf, H.; Willert-Porada, M. *J Power Sources* 2006, 153, 41.
22. Robberg, K.; Trapp, V. In *Handbook of Fuel Cells: Fundamentals, Technology, and Applications*; Vielstick, W.; Gasteiger, H. A.; Lamm, A., Eds.; Wiley: New York, 2003; Vol. 3, p 308.
23. Hermann, A.; Chaudhuri, T.; Spagnol, P. *Int J Hydrogen Energy* 2005, 30, 1297.
24. Wang, Y. M.Sc. Thesis, University of Waterloo, Waterloo, Ontario, Canada, 2006.
25. Dow Chemical Company. *The Dow Chemical Company Polypropylene Resin Product Literature, Form 167-00162-0905X*; Dow Chemical Company: Midland, MI, 2005.
26. Akzo Nobel. *Akzo Nobel Electrically Conductive Ketjenblack Product Literature*; Akzo Nobel: Chicago, IL, 1999.
27. Keith, J. M.; King, J. A.; Barton, R. L. *J Appl Polym Sci* 2006, 102, 3293.
28. Asbury Carbons. *Asbury Carbons Product Information*; Asbury Carbons: Asbury, NJ, 2004.
29. Conoco. *Conoco Carbons Products Literature*; Conoco, Inc.: Houston, TX, 1999.
30. Hyperion Catalysis International. *Hyperion Catalysis International Fibril Product Literature*; Hyperion Catalysis International: Cambridge, MA, 2008.
31. King, J. A.; Morrison, F. A.; Keith, J. M.; Miller, M. G.; Smith, R. C.; Cruz, M.; Neuhalfen, A. M.; Barton, R. L. *J Appl Polym Sci* 2006, 101, 2680.
32. Evaluating Thermal Conductivity of Gasket Materials, ASTM Standard D433-77 (Reapproved 1993), American Society for Testing and Materials, Philadelphia, 1996.
33. Heiser, J. A.; King, J. A.; Konell, J. P.; Miskioglu, I.; Sutter, L. L. *J Appl Polym Sci* 2004, 91, 2881.
34. Konell, J. P.; King, J. A.; Miskioglu, I. *Polym Compos* 2004, 25, 172.
35. King, J. A.; Barton, R. L.; Hauser, R. A.; Keith, J. M. *Polym Compos* 2008, 29, 421.
36. Weber, E. H.; Clingerman, M. L.; King, J. A. *J Appl Polym Sci* 2003, 88, 123.
37. Weber, E. H. Ph.D. Dissertation, Michigan Technological University, Houghton, MI, 2001.
38. Nielsen, L. *Ind Eng Chem Fundam* 1974, 13, 17.
39. McGee, S.; McCullough, R. L. *Polym Compos* 1981, 2, 149.
40. Keith, J. M.; King, J. A.; Lenhart, K. M.; Zimny, B. *J Appl Polym Sci* 2007, 105, 3309.
41. Hauser, R. A. Ph.D. Dissertation, Michigan Technological University, Houghton, MI, 2008.
42. Hone, J.; Whitney, M.; Piskoti, C.; Zettl, A. *Phys Rev B* 1999, 59, R2514.
43. Yi, W.; Lu, L.; Dian-Lin, Z.; Pan, Z. W.; Xie, S. S. *Phys Rev B* 1999, 59, R9015.
44. Hone, J.; Llaguno, M. C.; Nemes, N. M.; Johnson, A. T.; Fischer, J. E.; Walters, D. A.; Cassavant, M. J.; Schmidt, J.; Smalley, R. E. *Appl Phys Lett* 2000, 77, 666.
45. Kim, P.; Shi, L.; Majumdar, A.; McEuen, P. L. *Phys Rev Lett* 2001, 87, 215502.
46. Yang, D. J.; Zhang, Q.; Chen, G.; Yoon, S. F.; Ahn, J.; Wang, S. G.; Zhou, Q.; Wang, Q.; Li, J. Q. *Phys Rev B* 2002, 66, 165440.
47. King, J. A.; Tucker, K. W.; Vogt, B. D.; Weber, E. H.; Quan, C. *Polym Compos* 1999, 20, 643.
48. Miller, M. G. Ph.D. Dissertation, Michigan Technological University, Houghton, MI, 2006.
49. Hauser, R. A.; Keith, J. M.; King, J. A.; Holdren, J. L. *J Appl Polym Sci* 2008, 110, 2914.